

Axial anomaly in $^3\text{He-A}$: Simulation of Baryogenesis and Generation of primordial magnetic fields in Manchester and Helsinki

G.E. Volovik

*Low Temperature Laboratory, Helsinki University of Technology, Box 2200, FIN-02015 HUT, Finland
and*

Landau Institute for Theoretical Physics, Moscow, Russia

(February 2, 2020)

Keywords: superfluid ^3He , chiral anomaly, gap nodes, effective field theory, effective gravity

The gapless fermionic excitations in superfluid $^3\text{He-A}$ have a “relativistic” spectrum close to the gap nodes. They are the counterpart of chiral particles (left-handed and right-handed) in high energy physics above the electroweak transition. We discuss the effective gravity and effective gauge fields induced by these massless fermions in the low-energy corner. The interaction of the chiral fermions with the gauge field in $^3\text{He-A}$ is discussed in detail. It gives rise to the effect of axial anomaly: Conversion of charge from the coherent motion of the condensate (vacuum) to the quasiparticles (matter). The charge of the quasiparticles is thus not conserved. In other words, matter can be created without creating antimatter. This effect is instrumental for vortex dynamics, in which the vortex is the mediator of conversion of linear momentum from the condensate to the normal component via spectral flow in the vortex core. The same effect leads to the instability of the counterflow in $^3\text{He-A}$, in which the flow of the normal component (incoherent degrees of freedom) is transformed to the order parameter texture (coherent degrees of freedom). We discuss the analogues of these phenomena in high energy physics. The conversion of the momentum from the vortex to the heat bath is equivalent to the nonconservation of baryon number in the presence of textures and cosmic strings. The counterflow instability is equivalent to the generation of the hypermagnetic field via the axial anomaly. We discuss also an analogue of axions and different sources of the mass of the “hyperphoton” in $^3\text{He-A}$.

I. INTRODUCTION

A. Effective electrodynamics and gravity in $^3\text{He-A}$.

Many aspects of high energy physics can be modelled in condensed matter [1]. Superfluid $^3\text{He-A}$ provides a rich source for such a modelling. The most pronounced property of this superfluid is that in addition to the numerous bosonic fields (collective modes of the order parameter) it contains gapless fermionic quasiparticles. Close to the gap nodes, the points in momentum space where the energy is zero (Fig. 1), the energy spectrum of quasiparticles is linear in momentum \mathbf{p} . This simple circumstance has far-reaching consequences: The low energy fermions and some of the bosons obey “relativistic” equations, while their interaction with the superfluid vacuum mimics that of elementary particles with gauge fields. This illustrates the principle [2] that the effective physics in a low energy corner becomes more symmetric than in the general case. In $^3\text{He-A}$ we have two low energy corners, at $\mathbf{p} \approx \pm p_F \hat{\mathbf{l}}$, where p_F is the Fermi momentum and $\hat{\mathbf{l}}$ the unit vector specifying the direction of the nodes. This picture does not depend on details of the underlying microscopic interactions of atoms, whose only role is to produce values of “fundamental constants”, such as the “speed of light” and the “Planck energy”.

Close to the gap node the square of the quasiparticle energy E is generally a quadratic form of the deviation of the momentum \mathbf{p} from the position of the nodes $\pm p_F \hat{\mathbf{l}}$:

$$E_{\pm}^2(\mathbf{p}) = g^{ik}(p_i \mp p_F \hat{l}_i)(p_k \mp p_F \hat{l}_k). \quad (1)$$

Let us introduce an effective vector potential of the “electromagnetic field”

$$\mathbf{A} = p_F \hat{\mathbf{l}}, \quad (2)$$

and the “electric charge” e , with $e = +1$ for the quasiparticles in the vicinity of the node at $p_F \hat{\mathbf{l}}$ and $e = -1$ for the quasiparticles in the vicinity of the opposite node, at $-p_F \hat{\mathbf{l}}$. Then one obtains a spectrum of relativistic fermions moving on the gravitational and electromagnetic background, determined by the metric tensor g^{ik} and the vector potential \mathbf{A} :

$$E^2(\mathbf{p}) = g^{ik}(p_i - eA_i)(p_k - eA_k). \quad (3)$$

The symmetric matrix g^{ik} , which gives the contravariant components of the metric tensor, is generally determined by the directions of the principal axes forming the orthonormal basis ($\hat{\mathbf{e}}_1, \hat{\mathbf{e}}_2, \hat{\mathbf{e}}_3$) and by the “speeds of light” along these directions:

$$g^{ik} = c_1^2 \hat{e}_1^i \hat{e}_1^k + c_2^2 \hat{e}_2^i \hat{e}_2^k + c_3^2 \hat{e}_3^i \hat{e}_3^k. \quad (4)$$

It is important that the effective gauge field \mathbf{A} and the effective metric g^{ik} depend on space and time, since the order parameter in general and the $\hat{\mathbf{l}}$ -vector in particular are not fixed in $^3\text{He-A}$ and can form different types of textures. The quasiparticles view the order parameter textures as a curved Lorentzian space-time and *simultaneously* as gauge fields. These fields are dynamical: The

Effective Lagrangian for “electromagnetic” and “gravitational” fields can be obtained by integrating over the fermionic field. The same principle was used by Sakharov and Zeldovich to obtain an Effective Gravity [3] and Effective Electrodynamics [4] from vacuum fluctuations. In some special cases (and in this review we consider just such a case) the main contribution to the effective action comes from the vacuum fermions whose momenta \mathbf{p} are concentrated near the gap nodes, i.e. from the “relativistic” fermions. In these (and only in these) cases one obtains an effective Lagrangian which gives Maxwell equations for the \mathbf{A} -field. Since the “photons” are thus constructed from the fermionic degrees of freedom, the metric g^{ik} , which governs the propagation of “photons”, is the same as the metric governing the dynamics of the underlying fermionic quasiparticles. Following the title of the Laughlin talk at this Symposium, this provides an example of a “Gauge Theory from Nothing” [5].

From Eq.(3) it follows that $g^{00} = -1$ and $g^{0i} = 0$, but this is not the general case: Typically all the components of the dynamical metric tensor $g_{\mu\nu}$ depend on the position in space-time. In some cases the effective metric is not trivial giving rise to conical singularities [6], event horizons and ergoregions [7,8]. This also allows to simulate quantum gravity. Note that the primary quantities in this effective (quantum) gravity are the *contravariant* components $g^{\mu\nu}$. They appear in the low-energy corner of the fermionic spectrum and represent the low-energy properties of the quantum vacuum. The geometry of the effective space-time, in which the free quasiparticles follow a geodesic, is determined by the inverse metric $g_{\mu\nu}$ and thus is a secondary object. In a similar manner the effective Lorentzian space-time comes from the spectrum of the sound waves propagating on the background of a moving inhomogeneous liquid [9–11]. The difference to the case of superfluid liquid $^3\text{He-A}$ is that ordinary liquids are essentially dissipative classical systems and thus cannot serve as a model of the quantum vacuum.

The above mechanism of the generation of the gauge field \mathbf{A} and gravity $g^{\mu\nu}$ is valid for a general system with point gap nodes. In the particular case of $^3\text{He-A}$ the initial “nonrelativistic” fermionic spectrum has the form

$$E^2(\mathbf{p}) = v_F^2(p - p_F)^2 + \frac{\Delta_0^2}{p_F^2}(\hat{\mathbf{l}} \times \mathbf{p})^2, \quad (5)$$

where Δ_0 is the gap amplitude; $v_F = p_F/m^*$ is the Fermi velocity and m^* the effective mass of the quasiparticle in the normal Fermi-liquid state, which is typically about 3–6 times the bare mass m_3 of the ^3He atom.

In the low energy corner one obtains the “relativistic” spectrum of Eq. (3) with the following values of the “fundamental constants” [12,13]

$$c_1 = c_2 = \frac{\Delta_0}{p_F} \equiv c_\perp, \quad c_3 = v_F \equiv c_\parallel. \quad (6)$$

The space characterizing the motion of quasiparticles in $^3\text{He-A}$, i.e. the space in which the quasiparticles move along the geodesic curves (in the absence of other forces) has an uniaxial anisotropy, with the anisotropy axis along $\hat{\mathbf{l}}$:

$$\hat{\mathbf{e}}_3 = \hat{\mathbf{l}}. \quad (7)$$

The speed of a “light” along the $\hat{\mathbf{l}}$ -vector, c_\parallel , is about 3 orders of magnitude larger than that in the transverse direction: $c_\parallel \gg c_\perp$. Another important fundamental constant, Δ_0 , plays the role of the Planck energy cut-off, as will be illustrated later on.

B. Chiral fermions in $^3\text{He-A}$

The chiral properties of the fermionic spectrum is revealed after the square root of Eq. (3) is taken. This procedure is not unambiguous: One has to use the underlying BCS theory of Cooper pairing, which leads to the superfluid A-phase state in ^3He . In BCS theory one obtains the Bogoliubov-Nambu Hamiltonian for fermions, which in the low-energy corner transforms into the Weyl Hamiltonian for massless chiral particles. It is represented by the proper square root of Eq. (3):

$$\mathcal{H} = -e \sum_a c_a \tau^a \hat{e}_a^i (p_i - eA_i), \quad (8)$$

where τ^a are the Pauli matrices acting in the Bogoliubov-Nambu particle-hole space.

The more close inspection of the BCS theory for $^3\text{He-A}$ reveals that the order parameter contains 18 degrees of freedom and thus 18 propagating collective modes. Six of these collective modes, which represent propagating oscillations of position of nodes and of the slopes of the energy spectrum at the nodes, are shown in Fig. 2 together with their analogs in relativistic theories.

The important property of this Hamiltonian is that the sign of the “electric” charge e simultaneously determines the chirality of the fermions. This is clearly seen with a simple isotropic example having $c_1 = c_2 = c_3 = c$:

$$\mathcal{H} = -ec\vec{\tau} \cdot (\mathbf{p} - e\mathbf{A}). \quad (9)$$

A particle with positive (negative) e is left-handed (right-handed): Its Bogoliubov spin $\vec{\tau}$ is antiparallel (parallel) to the momentum \mathbf{p} , if \mathcal{H} is positive definite. Thus the field \mathbf{A} corresponds to the axial field in relativistic theories. The symmetry between left and right is broken in $^3\text{He-A}$.

Rather few systems have (3+1)-dimensional chiral fermions as excitations. The superfluid $^3\text{He-A}$ and the Standard Model of the electroweak interactions are among these exotic systems. This is why $^3\text{He-A}$ is the best condensed matter system for the simulation of effects

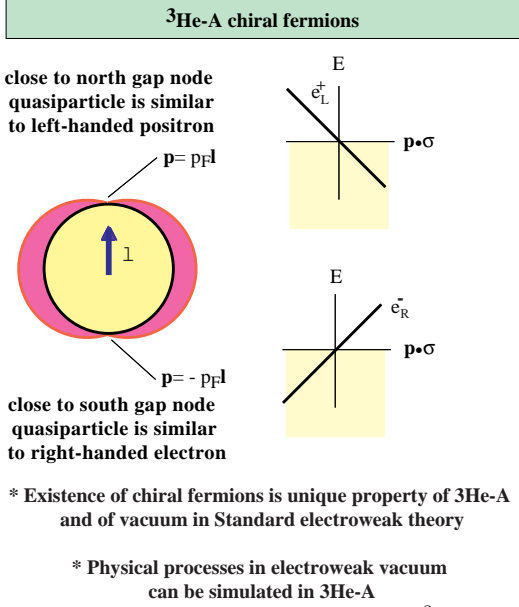


FIG. 1. Gap nodes and chiral fermions in ${}^3\text{He-A}$. Close to the gap nodes the gapless quasiparticles correspond to massless fermions moving in electromagnetic and gravity fields and obey relativistic equations. The left-handed particles have positive charge $e = +1$ and are in the vicinity of the north pole, as determined by the direction of the $\hat{\mathbf{l}}$ -vector, while the right particles with $e = -1$ are in the vicinity of the south pole. If the $\hat{\mathbf{l}}$ -field is not uniform in space and time, the space and time derivatives of $\mathbf{A} = p_F \hat{\mathbf{l}}$ act on the quasiparticle similar to magnetic and electric fields.

related to the chiral nature of the fermions, especially of the chiral anomaly. There are other condensed matter systems with chiral fermions, but these fermions occupy a space-time of 2+1 or 1+1 dimensions. Examples are the (2+1)-dimensional fermions in high-temperature superconductors [14]; (1+1)-dimensional chiral edge states in the quantum Hall effect [15,16], and in superconductors with broken time-reversal symmetry [17,18]. Finally fermionic excitations in the core of quantized vortices bear this property, too [8]. The gap nodes in (3+1)-dimensional theories can appear also in different types of “color superfluidity” – quark condensates in dense baryonic matter [19].

The spectrum of fermionic excitations of the electroweak vacuum in the present Universe contains one branch of chiral particles: The left-handed neutrino branch (Fig. 3). The right-handed neutrino is not present (or interacts with other matter different from the left-handed one). This is a remarkable manifestation of the violation of the left-right symmetry in the electroweak vacuum. Another symmetry, which is broken in the present Universe, is the $SU(2)$ symmetry of weak interactions. In the symmetric state of the early Universe, the left leptons (neutrino and left electron) formed a

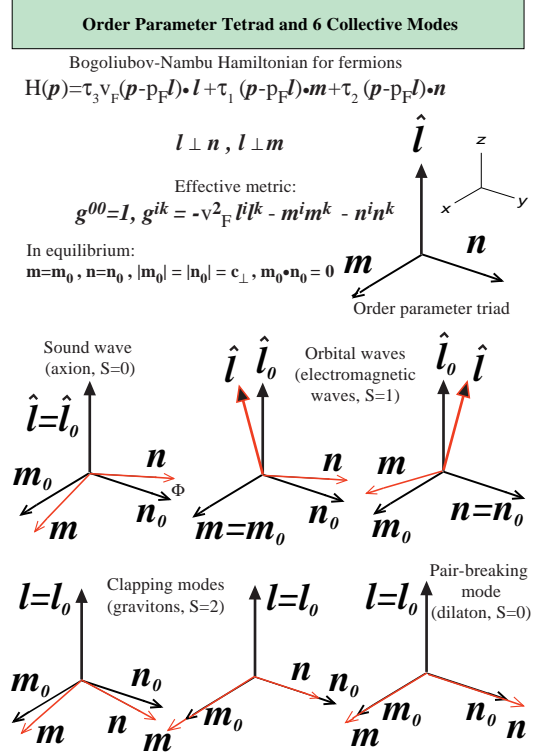


FIG. 2. Triads \mathbf{m}, \mathbf{n} and $\hat{\mathbf{l}} \propto \mathbf{m} \times \mathbf{n}$, which characterize the order parameter in ${}^3\text{He-A}$ for a given spin projection. The dynamics of two vector fields \mathbf{m} and \mathbf{n} gives rise to 6 collective modes: (1) Sound wave (axion) is propagating rotational oscillations of the triad around the $\hat{\mathbf{l}}$ vector. The angle Φ of this rotation is the phase of the superfluid condensate, whose gradient determines the superfluid velocity; (2-3) Orbital waves (photons) are propagating oscillations of the direction of the $\hat{\mathbf{l}}$ vector; (4-5) Clapping modes (gravitons) are out-of-phase oscillations of the diad \mathbf{m}, \mathbf{n} ; and (6) Pair-breaking mode (dilaton) is the oscillation of the modulus of the \mathbf{m} and \mathbf{n} vectors. This corresponds to the propagating oscillations of the transverse speed of light c_\perp . If the spin degrees of freedom are taken into account, the number of collective modes is triplicated.

$SU(2)$ doublet, while the right electron is in a $SU(2)$ singlet. During the cooldown of the Universe the phase transition occurred, at which the $SU(2) \times U(1)$ symmetry was broken to the electromagnetic $U(1)$ symmetry. As a consequence, the left and right electrons were hybridized forming the present electronic spectrum with the gap $\Delta = m_e c^2$. The electric properties of the vacuum thus exhibited the metal-insulator phase transition: The “metallic” state of the vacuum with the Fermi point in the electronic spectrum was transformed to the insulating state with the gap. Recent numerical calculations suggest that this transformation occurs either by the first order phase transition or by continuous cross-over without any real symmetry breaking [20].

The similarity between the chiral fermions in electroweak theory and in ${}^3\text{He-A}$ has also a topological origin. The gap nodes – zeroes in the particle (quasiparticle) spectrum – are characterized by a topological invariant in 4-momentum space belonging to the third homotopy group π_3 [12]:

$$N_{\text{top}} = \frac{1}{24\pi^2} \epsilon_{\mu\nu\lambda\gamma} \text{tr} \int_{\sigma} dS^{\gamma} \mathcal{G} \partial_{p^{\mu}} \mathcal{G}^{-1} \mathcal{G} \partial_{p^{\nu}} \mathcal{G}^{-1} \mathcal{G} \partial_{p^{\lambda}} \mathcal{G}^{-1}. \quad (10)$$

Here

$$\mathcal{G}(p_{\mu}) = \frac{1}{ip_0 + \mathcal{H}} \quad (11)$$

is the Green's function and σ is the 3-dimensional surface around the point node in the 4-momentum space. For the relativistic chiral particle the node is at $p_0 = 0$, $\mathbf{p} = 0$, while in ${}^3\text{He-A}$ the nodes are at $p_0 = 0$, $\mathbf{p} = \pm p_F \hat{\mathbf{l}}$. In all cases the topological invariant is nonzero: $N_{\text{top}} = \pm 1$, and the sign of N_{top} depends on chirality.

The topological stability – the conservation of the topological invariant in Eq. (10) – is important for the fermionic system. It implies that under a deformation of the system (under a continuous change of the system parameters) the gap nodes in momentum space can arise or disappear only in pairs (node-“antinode” pairs). This topological stability, which does not depend on the details and the symmetry of the system, provides topological conservation of chirality: The algebraic number of the chiral fermions, i.e. the number of the right fermionic species minus the number of the left fermionic species, is conserved: $\Delta N = N_{FR} - N_{FL} = \sum N_{\text{top}}$. In ${}^3\text{He-A}$ one has $N_{FR} = N_{FL} = 1$ and thus $\Delta N = \sum N_{\text{top}} = 0$.

In the relativistic theories the electroweak transition $SU(2) \times U(1) \rightarrow U(1)$ satisfies this topological rule: If the right neutrinos are absent, the algebraic number of chiral fermions per each generation is $\Delta N = -1$ in both phases: in the symmetric phase $SU(2) \times U(1)$ one has $\Delta N = 7 - 8 = -1$ and in the broken symmetry phase $U(1)$ one has $\Delta N = 0 - 1 = -1$. In this case the conservation of the topological invariant provides the zero mass for neutrino. In the unification theories, the $SU(5)$ symmetry breaking pattern with $N_{FL} = 10 + 5$ left fermions in one generation does not satisfy this topological rule. The rule holds only if one doubles the number of fermions and considers right antiparticles as independent particles: in this case $\Delta N = 15 - 15 = 0$. In the $SU(4) \times SU_L(2) \times SU_R(2)$ theory with $N_{FR} = N_{FL} = 8$ the topological rule is satisfied without the doubling of fermions: one has $\Delta N = 0$ throughout all the route of the symmetry breaking to $SU(3) \times U(1)$.

II. AXIAL ANOMALY

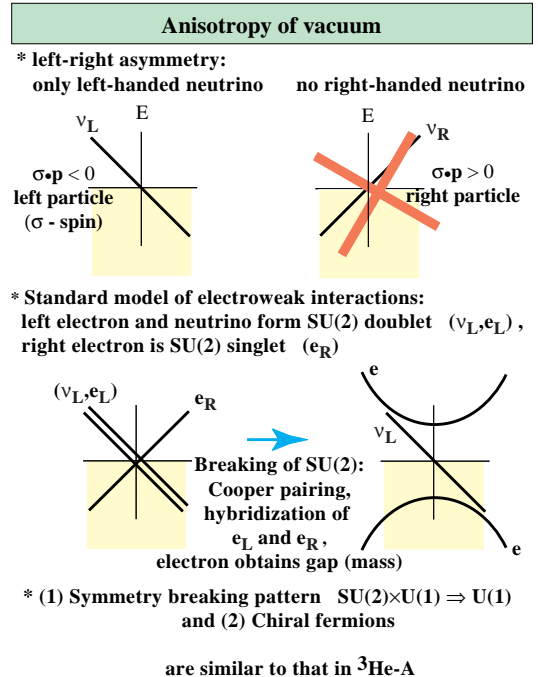


FIG. 3. (*top*): The spectrum of fermionic excitations of the physical vacuum contains a branch of chiral particles, the left-handed neutrino branch. The right-handed neutrino does not exist (or interacts with other matter only via the gravitational field). In the symmetric state of the early Universe, the left leptons (neutrino and left electron) formed the $SU(2)$ doublet, while the right electron was the $SU(2)$ singlet. (*bottom*): During the cool down of the Universe the $SU(2)$ symmetry was broken in a phase transition. The left and right electrons were hybridized forming the present electronic spectrum with the gap $\Delta = m_e c^2$. The electric properties of the vacuum thus exhibited the metal-insulator transition.

A. Adler-Bell-Jackiw equation

Chiral fermions interacting with gauge fields exhibit the effect of chiral anomaly, the nonconservation of matter charge due to the interaction of matter with the quantum vacuum. The origin for the axial anomaly can be seen from the behavior of the chiral particle in a constant magnetic field, $\mathbf{A} = (1/2)\mathbf{B} \times \mathbf{r}$. The Hamiltonians for the right particle with the electric charge e_R and for the left particle with the electric charge e_L are

$$\mathcal{H} = c\vec{\tau} \cdot (\mathbf{p} - e_R \mathbf{A}), \quad \mathcal{H} = -c\vec{\tau} \cdot (\mathbf{p} - e_L \mathbf{A}). \quad (12)$$

Fig. 4 shows the energy spectrum in a magnetic field \mathbf{B} along z ; the thick lines show the occupied negative-energy states. Motion of the particles in the plane perpendicular to \mathbf{B} is quantized into the Landau levels shown. The free motion is thus effectively reduced to one-dimensional motion along \mathbf{B} with momentum p_z . Because of the chirality of the particles the lowest ($n = 0$) Landau level is asym-

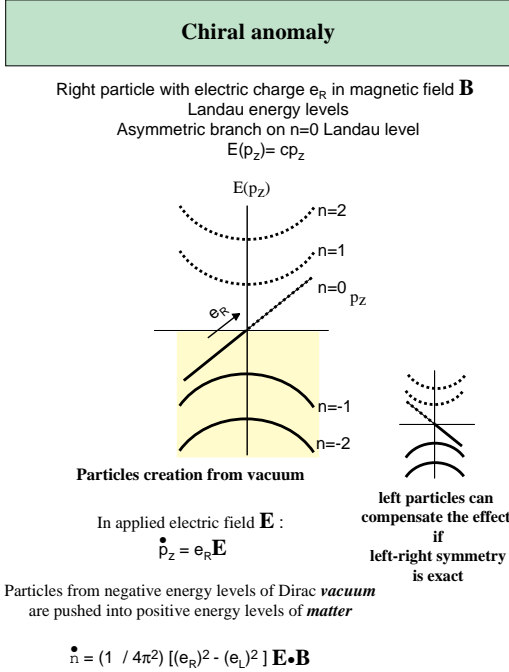


FIG. 4. Chiral anomaly: the spectral flow from the occupied energy levels caused by the applied electric field leads to the creation of the fermionic charge from the vacuum if the left-right symmetry is violated.

metric. It crosses zero only in one direction: $E = cp_z$ for the right particle and $E = -cp_z$ for the left one. If we now apply an electric field \mathbf{E} along z , particles are pushed from negative to positive energy levels according to the equation of motion $\dot{p}_z = e_R E_z$ ($\dot{p}_z = e_L E_z$) and the whole Dirac sea moves up (down) creating particles and electric charge from the vacuum. This motion of particles along the “anomalous” branch of the spectrum is called *spectral flow*. The rate of particle production is proportional to the density of states at the Landau level, which is $\propto |e_R \mathbf{B}|$ ($|e_L \mathbf{B}|$), so that the rate of production of particle number $n = n_R + n_L$ and of charge $Q = n_R e_R + n_L e_L$ from the vacuum is

$$\dot{n} = \frac{1}{4\pi^2} (e_R^2 - e_L^2) \mathbf{E} \cdot \mathbf{B}, \quad \dot{Q} = \frac{1}{4\pi^2} (e_R^3 - e_L^3) \mathbf{E} \cdot \mathbf{B}. \quad (13)$$

This is an anomaly equation for the production of particles from vacuum of the type found by Adler [21] and by Bell and Jackiw [22] in the context of neutral pion decay. We see that for particle or charge creation from “nothing” it is necessary to have an asymmetric branch of the dispersion relation $E(p)$ which crosses the axis from negative to positive energy. Additionally, the symmetry between the left and right particles has to be violated:

$e_R \neq e_L$ for the charge creation and $e_R^2 \neq e_L^2$ for the particle creation.

B. Anomalous nucleation of baryonic charge

In the standard electroweak model there is an additional accidental global symmetry $U(1)_B$ whose classically conserved charge is the baryon number Q_B . Each of the quarks is assigned $Q_B = 1/3$ while the leptons (neutrino and electron) have $Q_B = 0$. This baryonic number is not conserved due to the axial anomaly. There are two gauge fields whose “electric” and “magnetic” fields become a source for baryoproduction: The hypercharge field $U(1)$ and the weak field $SU(2)$. The corresponding hypercharges Y and weak charges W of the left u and d quarks are

$$Y_{dL} = Y_{uL} = 1/6, \quad W_{dL} = -W_{uL} = 1/2, \quad (14)$$

whereas for the right u and d quarks one has

$$Y_{uR} = 2/3, \quad Y_{dR} = -1/3, \quad W_{dR} = W_{uR} = 0. \quad (15)$$

Let us first consider the effect of the hypercharge field. Since the number of different species of quarks carrying the baryonic charge is $3N_F$ (3 colours $\times N_F$ generations of fermions) and the baryonic charge of the quark is $Q_B = 1/3$, the production rate of baryonic charge in the presence of hyperelectric and hypermagnetic fields is

$$\frac{N_F}{4\pi^2} (Y_{dR}^2 + Y_{uR}^2 - Y_{dL}^2 - Y_{uL}^2) \mathbf{B}_Y \cdot \mathbf{E}_Y. \quad (16)$$

Since the hypercharges of left and right quarks are different (see Eqs. (14,15)), one obtains a nonzero production of baryons by the hypercharge field

$$\frac{N_F}{8\pi^2} \mathbf{B}_Y \cdot \mathbf{E}_Y. \quad (17)$$

The weak electric and magnetic fields also contribute to the production of the baryonic charge:

$$\frac{N_F}{4\pi^2} (W_{dR}^2 + W_{uR}^2 - W_{dL}^2 - W_{uL}^2) \mathbf{B}_W^a \cdot \mathbf{E}_{aW}, \quad (18)$$

which gives

$$-\frac{N_F}{8\pi^2} \mathbf{B}_W^a \cdot \mathbf{E}_{aW}. \quad (19)$$

Thus the total rate of baryon production in the Standard model takes the form

$$\dot{Q}_B = \frac{N_F}{8\pi^2} (-\mathbf{B}_W^a \cdot \mathbf{E}_{aW} + \mathbf{B}_Y \cdot \mathbf{E}_Y). \quad (20)$$

The first term comes from nonabelian $SU(2)$ fields, it shows that the nucleation of baryons occurs when the topological charge of the vacuum changes, say, by sphaleron or due to de-linking of linked loops of the cosmic strings. The second, nontopological, term describes the exchange of the baryonic charge between the hypermagnetic field and the fermionic degrees of freedom.

C. Anomalous nucleation of linear momentum in ${}^3\text{He-A}$

The anomaly equation which describes the nucleation of fermionic charges in the presence of magnetic and electric fields describes both the production of the baryons in the electroweak vacuum (baryogenesis) and the production of the linear momentum in the superfluid ${}^3\text{He-A}$ (momentogenesis). In ${}^3\text{He-A}$ the effective $U(1)$ gauge field is generated by the moving $\hat{\mathbf{l}}$ -texture. According to Eq. (2), the time and space dependent $\hat{\mathbf{l}}$ vector, associated with the motion of the so-called continuous vortex (see below), produces a force on the excitations equivalent to that of an “electric” (or “hyperelectric”) field $\mathbf{E} = p_F \partial_t \hat{\mathbf{l}}$ and a “magnetic” (or “hypermagnetic”) field $\mathbf{B} = p_F \nabla \times \hat{\mathbf{l}}$ acting on particles of unit charge. Equation (13) can then be applied to calculate the rate at which left-handed and right-handed quasiparticles are created by spectral flow. What we are interested in is the production of the particle momentum due to spectral flow:

$$\dot{\mathbf{P}} = \frac{1}{4\pi^2} (\mathbf{P}_R - \mathbf{P}_L) (\mathbf{E} \cdot \mathbf{B}) . \quad (21)$$

Since the right and left particle have opposite momenta $\mathbf{P}_R = p_F \hat{\mathbf{l}} = -\mathbf{P}_L$, excitation momentum is created at a rate

$$\dot{\mathbf{P}} = \frac{p_F^3}{2\pi^2} \hat{\mathbf{l}} (\partial_t \hat{\mathbf{l}} \cdot (\vec{\nabla} \times \hat{\mathbf{l}})) . \quad (22)$$

However, the total linear momentum of the liquid has to be conserved. Therefore Eq. (22) implies that in the presence of a time-dependent texture momentum is transferred from the superfluid ground state (analogue of vacuum) to the heat bath of excitations forming the normal component (analogue of matter).

III. SPECTRAL FLOW FORCE ON VORTEX

A. Continuous vortex and baryogenesis in textures

The anomalous production of linear momentum leads to an additional force acting on the continuous vortex in ${}^3\text{He-A}$ (Fig. 5).

The continuous vortex, first discussed by Chechetkin [23] and Anderson and Toulouse [24] (ATC vortex), has in its simplest realization the following distribution of the $\hat{\mathbf{l}}$ -field ($\hat{\mathbf{z}}$, $\hat{\mathbf{r}}$ and $\hat{\phi}$ are unit vectors of the cylindrical coordinate system)

$$\hat{\mathbf{l}}(r, \phi) = \hat{\mathbf{z}} \cos \eta(r) + \hat{\mathbf{r}} \sin \eta(r) , \quad (23)$$

where $\eta(r)$ changes from $\eta(0) = \pi$ to $\eta(\infty) = 0$ in the so called soft core of the vortex. The superfluid velocity \mathbf{v}_s in superfluid ${}^3\text{He-A}$ is determined by the twist of the

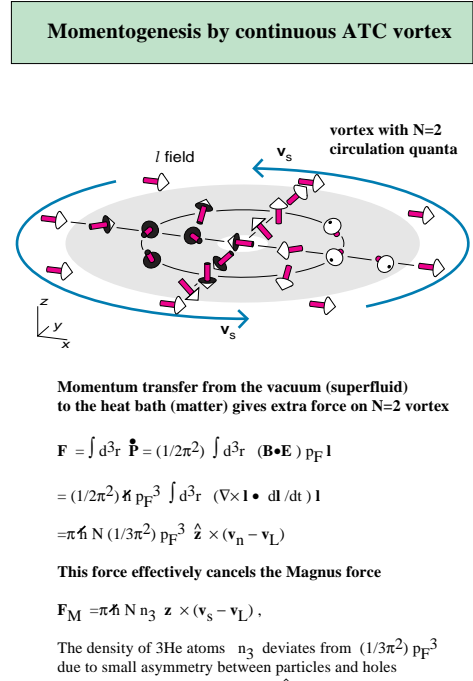


FIG. 5. The order parameter $\hat{\mathbf{l}}$ -texture (analogue of the vector potential of the (hyper) electromagnetic field) in the soft core of the continuous Anderson-Toulouse-Chechetkin vortex [23,24] (ATC vortex). The moving vortex converts the textural (vacuum) fermionic charge (linear momentum) to fermionic quasiparticles (matter). The moving vortex generates the time dependence of the order parameter, which is equivalent to an electric field \mathbf{E} . Together with the effective magnetic field \mathbf{B} concentrated in the soft core of the ATC vortex this gives rise to a nonzero dot product $\mathbf{B} \cdot \mathbf{E}$, which is the anomalous source of fermionic charge.

triad $\hat{\mathbf{e}}_1, \hat{\mathbf{e}}_2, \hat{\mathbf{e}}_3$ and corresponds to torsion in the tetrad formalism of gravity (the space-time dependent rotation of vectors $\mathbf{m} = c_\perp \hat{\mathbf{e}}_1$ and $\mathbf{n} = c_\perp \hat{\mathbf{e}}_2$ about axis $\hat{\mathbf{l}}$ in Fig. 2):

$$\mathbf{v}_s = \frac{\hbar}{2m_3} \hat{\mathbf{e}}_1^i \vec{\nabla} \hat{\mathbf{e}}_2^i . \quad (24)$$

In comparison to a more familiar singular vortex, the continuous vortex has a regular superfluid velocity field

$$\mathbf{v}_s(r, \phi) = -\frac{\hbar}{2m_3 r} [1 + \cos \eta(r)] \hat{\phi} , \quad (25)$$

with no singularity on the vortex axis.

The stationary vortex generates a “magnetic” field. If the vortex moves with a constant velocity \mathbf{v}_L it also generates an “electric” field, since $\hat{\mathbf{l}}$ depends on $\mathbf{r} - \mathbf{v}_L t$:

$$\mathbf{B} = p_F \vec{\nabla} \times \hat{\mathbf{l}} , \quad \mathbf{E} = \partial_t \mathbf{A} = -p_F (\mathbf{v}_L \cdot \vec{\nabla}) \hat{\mathbf{l}} \quad (26)$$

The net production of the quasiparticle momenta by the spectral flow in the moving vortex means, if the vortex moves with respect to the system of quasiparticles

(the normal component of liquid or matter, whose flow is characterised by the normal velocity \mathbf{v}_n), that there is a force acting between the normal component and the vortex. Integration of the anomalous momentum transfer in Eq.(22) over the cross-section of the soft core of the moving ATC vortex gives the following force acting on the vortex (per unit length) from the system of quasi-particles [25]:

$$\mathbf{F}_{sf} = \int d^2r \frac{p_F^3}{2\pi^2} \hat{\mathbf{I}} (\partial_t \hat{\mathbf{I}} \cdot (\vec{\nabla} \times \hat{\mathbf{I}})) = -2\pi\hbar C_0 \hat{\mathbf{z}} \times (\mathbf{v}_L - \mathbf{v}_n), \quad (27)$$

where

$$C_0 = p_F^3/3\pi^2. \quad (28)$$

Note that this spectral-flow force is transverse to the relative motion of the vortex and thus is nondissipative (reversible). In this derivation it was assumed that the quasiparticles and their momenta, created by the spectral flow from the vacuum, are finally absorbed by the normal component. The time delay in the process of absorption and also the viscosity of the normal component lead to a dissipative (friction) force between the vortex and the normal component: $\mathbf{F}_{fr} = -\gamma(\mathbf{v}_L - \mathbf{v}_n)$. There is no momentum exchange between the vortex and the normal component if they move with the same velocity.

Another important property of the spectral-flow force (27) is that it does not depend on the details of the vortex structure: The result for \mathbf{F}_{sf} is robust against any deformation of the $\hat{\mathbf{I}}$ -texture which does not change the asymptote, i.e. the topology of the vortex. In this respect this force resembles another force, which acts on the vortex moves with respect to the superfluid vacuum. This is the well-known Magnus force:

$$\mathbf{F}_M = 2\pi\hbar n_3 \hat{\mathbf{z}} \times (\mathbf{v}_L - \mathbf{v}_s(\infty)). \quad (29)$$

Here n_3 is the particle density (here the number density of ^3He atoms) and $\mathbf{v}_s(\infty)$ is the uniform velocity of the superfluid vacuum far from the vortex.

The balance between all the forces acting on the vortex, \mathbf{F}_{sf} , \mathbf{F}_{fr} , \mathbf{F}_M and some other forces, including any external force and the so-called Iordanskii force coming from the gravitational analog of the Aharonov-Bohm effect [26], determines the velocity of the vortex and causes it to be a linear combination of $\mathbf{v}_s(\infty)$ and \mathbf{v}_n . Due to this balance the fermionic charge (the linear momentum), which is transferred from the fermionic heat bath to the vortex texture, is further transferred from the vortex texture to the superfluid motion. Thus the vortex texture serves as intermediate object for the momentum exchange between the fermionic matter and the superfluid vacuum. In this respect the texture corresponds to the sphaleron or to the cosmic string in relativistic theories.

The result (27) for the spectral-flow force, derived for the ATC vortex from the axial anomaly equation (22), was confirmed in a microscopic theory, which took into account the discreteness of the quasiparticle spectrum in the soft core [27]. This was also confirmed in experiments on vortex dynamics in $^3\text{He-A}$ [28,29].

In such experiments a uniform array of vortices is produced by rotating the whole cryostat. In equilibrium the vortices and the normal component (heat bath) of the fluid rotate together with the cryostat. An electrostatically driven vibrating diaphragm produces an oscillating superflow, which via the Magnus force generates the vortex motion, while the normal component remains clamped due to its high viscosity. This creates a motion of vortices with respect both to the heat bath and the superfluid vacuum. The vortex velocity \mathbf{v}_L is determined by the overall balance of forces acting on the vortices, which in the absence of the external forces can be expressed in terms of the two parameters, so-called mutual friction parameters: [28]

$$\hat{\mathbf{z}} \times (\mathbf{v}_L - \mathbf{v}_s(\infty)) + d_\perp \hat{\mathbf{z}} \times (\mathbf{v}_n - \mathbf{v}_L) + d_\parallel (\mathbf{v}_n - \mathbf{v}_L) = 0. \quad (30)$$

Measurement of the damping of the diaphragm resonance and of the coupling between different eigenmodes of vibrations enables both parameters, d_\perp and d_\parallel , to be deduced.

From the above theory of spectral flow in the $^3\text{He-A}$ vortex texture it follows that the parameter, which characterizes the transverse forces acting on the vortex, is given by

$$d_\perp \approx \frac{C_0 - n_3 + n_s(T)}{n_s(T)}, \quad (31)$$

where $n_s(T)$ is the density of the superfluid component. In this equation the parameter C_0 from Eq.(28) arises through the axial anomaly, the particle density n_3 stems from the Magnus force and the superfluid density $n_s(T)$ from the combined effect of Magnus and Iordanskii forces. The effect of the chiral anomaly is crucial for the parameter d_\perp since C_0 is comparable with n_3 , since $C_0 = p_F^3/3\pi^2$ is the particle density of liquid ^3He in the normal state. The difference between C_0 and n_3 is thus determined by the tiny effect of superfluidity on the particle density and is extremely small: $n_3 - C_0 \sim n_3(\Delta_0/v_F p_F)^2 = n_3(c_\perp/c_\parallel)^2 \ll n_3$. Because of the axial anomaly one must have $d_\perp \approx 1$ for all practical temperatures, even including the region close to T_c , where the superfluid component $n_s(T) \sim n_3(1 - T^2/T_c^2)$ is small. $^3\text{He-A}$ experiments, made in the whole temperature range where $^3\text{He-A}$ is stable, gave precisely this value within experimental uncertainty, $|1 - d_\perp| < 0.005$ [28].

This provides an experimental verification of the Adler-Bell-Jackiw axial anomaly equation (13), applied

to ${}^3\text{He-A}$, and thus supports the idea that baryonic charge (and also leptonic charge) can be generated by electroweak fields.

B. Singular vortex and baryogenesis by cosmic strings

There are many different scenarios of the electroweak baryogenesis [30,31]. In some of them the baryonic charge is created in the cores of topological objects, in particular in the core of cosmic strings. While a weak and hypercharge magnetic flux is always present in the core of electroweak strings, a weak and hypercharge electric field can be present along the string if the string is moving across a background electromagnetic field [32] or in certain other processes such as the de-linking of two linked loops [33,34]. Parallel electric and magnetic fields in the string change the baryonic charge and can lead to cosmological baryogenesis [35] and to the presence of antimatter in cosmic rays [36].

Again the axial anomaly is instrumental for the baryoproduction in the core of cosmic strings. But now the effect cannot be described by the anomaly equation (13). This equation was derived using the energy spectrum of the free massless fermions in the presence of the homogeneous electric and magnetic fields. But in cosmic strings these fields are no more homogeneous. Moreover the massless fermions exist only in the vortex core as bound states in the potential well produced by the order parameter (Higgs) field. Thus the consideration of baryoproduction should be essentially different: the spectral flow phenomenon has to be studied using an exact spectrum of the massless bound states, namely fermion zero modes on strings.

A similar situation takes place in condensed matter, where the counterpart of the cosmic string is the conventional quantized vortex with a singular core (Fig. 6). The vortices with singular cores are: (i) Abrikosov vortices in superconductors; (ii) vortices in superfluid ${}^3\text{He-B}$; and (iii) such vortices in ${}^3\text{He-A}$ which, as distinct from the continuous vortices, belong to the nontrivial elements of the π_1 homotopy group. It appears that the momentogenesis due to the axial anomaly also takes place here, but as distinct from the case of the continuous ATC vortex in ${}^3\text{He-A}$, it cannot be described by the continuous anomaly equation of the type of Eq. (21). For its description one should consider the spectral properties of the fermion zero modes localized in the singular vortex core. The main difference between fermion zero modes in relativistic strings and in the conventional condensed matter vortices is the following. In strings the anomalous branch $E(p_z)$ which crosses zero and gives rise to the spectral flow from the negative vacuum energy levels to the positive matter energy levels of is given in terms of a continuous variable – the linear momentum p_z along

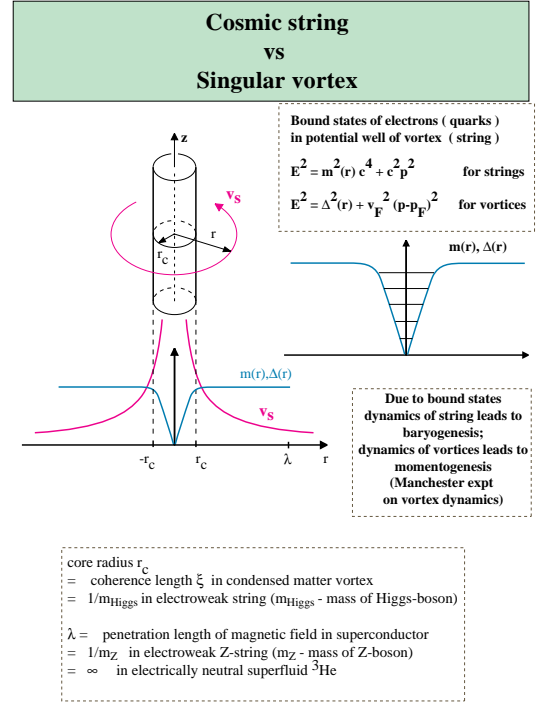


FIG. 6. A cosmic string is the counterpart of the Abrikosov vortex in superconductors. It also supports bound states of the fermions, which is important for the electroweak baryoproduction.

the string. In contrast, in the case of condensed-matter vortices (Fig. 7) the branch $E(L_z)$ is “crossing” zero as a function of the *discrete* angular momentum $\hbar L_z$ (L_z can be integral or half-odd integral). The level flow along the discrete energy levels is suppressed and is determined by the interlevel distance $\hbar\omega_0$ and the level width \hbar/τ resulting from the scattering of core excitations by free excitations in the heat bath outside the core (or by impurities in superconductors).

This suppression of spectral flow results in a renormalization of the spectral-flow parameter, which is roughly [37,38]

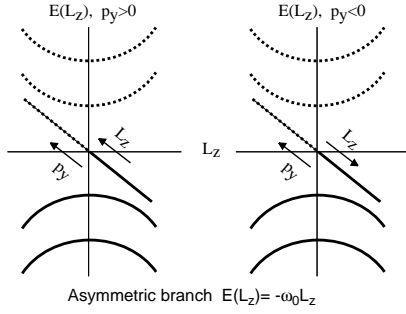
$$\tilde{C}_0 \sim \frac{C_0}{1 + \omega_0^2 \tau^2}, \quad (32)$$

and the Eq. (31) becomes:

$$d_{\perp} \approx \frac{\tilde{C}_0 - n_3 + n_s(T)}{n_s(T)} \quad (33)$$

If $\omega_0 \tau \ll 1$, the levels overlap and spectral flow is allowed. In the opposite limit $\omega_0 \tau \gg 1$ it is completely suppressed. The parameter $\omega_0 \tau$ depends on temperature and this allows us to check Eq. (33) experimentally. This has been done in an experiment in Manchester on the dynamics of singular vortices in ${}^3\text{He-B}$ [28,29]. An equation

**Anomalous nonconservation of linear momentum
in superconductors and in $^3\text{He-B}$ vortex**



When vortex moves along x the angular momentum changes

$$\dot{L}_z = \dot{x} p_y = v_x p_y$$

This gives the flow of levels from Fermi sea

$$\dot{n} = \dot{L}_z / \hbar = v_x p_y / \hbar$$

The flow of linear momentum (transverse force on vortex)

$$\begin{aligned} F_y &= \langle \dot{p}_y \rangle = \langle p_y \dot{n} \rangle = \langle p_y^2 \rangle v_x / \hbar = \\ &= \pi \hbar (1/3\pi^2) p_F^3 v_x \end{aligned}$$

FIG. 7. Spectral flow of momentum in the core of the moving singular vortex leads to the experimentally observed reactive force on a vortex in superfluid $^3\text{He-B}$.

of the type of (33) has been verified in a broad temperature range, which included both extreme limits, $\omega_0 \tau \ll 1$ and $\omega_0 \tau \gg 1$.

IV. MAGNETIC FIELD FROM FERMIONIC CHARGE

A recent scenario of the generation of primordial magnetic fields by Joyce and Shaposhnikov [39,40] is based on an effect, which is the inverse to that discussed in the previous section. The axial anomaly gives rise to a transformation of an excess of chiral particles into a hypermagnetic field. In $^3\text{He-A}$ language this process describes the collapse of excitation momenta (fermionic charges) towards the formation of textures. These textures are the counterpart of the hypermagnetic field in the Joyce-Shaposhnikov scenario [41] (Figs. 8,9). Such a collapse of quasiparticle momentum was recently observed in the rotating cryostat of the Helsinki Low Temperature Laboratory [42,41].

A. Effective Lagrangian at low T

To study the instability of the superflow and relate it to the problem of magnetogenesis, let us start with

the relevant Effective Lagrangian for superfluid dynamics at low T and find the correspondence to the effective Lagrangian for the system of chiral fermions interacting with the magnetic or hypermagnetic field via the axial anomaly conversion process. For the hydrodynamic action in $^3\text{He-A}$ we shall use the known results collected in the book [43].

Consider a superfluid moving with respect to the walls of container. The normal component of the liquid is clamped by the vessel walls due to its high viscosity, so that the normal velocity $\mathbf{v}_n = 0$ in the reference frame moving with the vessel. If the superfluid velocity \mathbf{v}_s of the condensate in Eq. (24) is nonzero in this reference frame, one has a nonzero counterflow of the superfluid and normal components with relative velocity $\mathbf{w} = \mathbf{v}_s - \mathbf{v}_n$. This relative velocity provides a nonzero fermionic charge of matter, as will be seen below, and the flow instability leads to the transformation of this charge to the analogue of the hypermagnetic field. Let us choose the axis z along the velocity \mathbf{w} of the counterflow. In equilibrium the unit orbital vector $\hat{\mathbf{l}}$ is oriented along the counterflow: $\hat{\mathbf{l}}_0 = \hat{\mathbf{z}}$. The stability problem is investigated using the quadratic form of the deviations of the superfluid velocity and the $\hat{\mathbf{l}}$ -vector from their equilibrium values:

$$\hat{\mathbf{l}} = \hat{\mathbf{l}}_0 + \delta\hat{\mathbf{l}}(\mathbf{r}, t) - \frac{1}{2}\hat{\mathbf{l}}_0(\delta\hat{\mathbf{l}}(\mathbf{r}, t))^2, \quad \mathbf{v}_s = \mathbf{w}_0 + \delta\mathbf{v}_s(\mathbf{r}, t). \quad (34)$$

The instability of the counterflow towards generation of the inhomogeneity $\delta\hat{\mathbf{l}}(\mathbf{r}, t)$, corresponds to the generation of the magnetic field $\mathbf{B} = p_F \nabla \times \delta\hat{\mathbf{l}}$ from the chiral fermions.

There are 3 terms in the energy of the liquid, which are relevant for our consideration of stability of superflow at low T :

$$\begin{aligned} F &= \frac{1}{2} m_3 n_s^{ij} v_{si} v_{sj} + C_0 (\mathbf{v}_s \cdot \hat{\mathbf{l}}) (\hat{\mathbf{l}} \cdot (\nabla \times \hat{\mathbf{l}})) \\ &\quad + K_b (\hat{\mathbf{l}} \times (\nabla \times \hat{\mathbf{l}}))^2 \end{aligned} \quad (35)$$

(1) The first term in Eq. (35) is the kinetic energy of superflow with n_s^{ij} being the anisotropic tensor of superfluid density. At low T one has

$$n_s^{ij} \approx n_3 \delta^{ij} - n_{n\parallel} \hat{l}^i \hat{l}^j, \quad n_{n\parallel} \approx \frac{m^*}{3m_3} p_F^3 \frac{T^2}{\Delta_0^2}. \quad (36)$$

(2) The second term in Eq. (35) is the anomalous interaction of the superflow with the $\hat{\mathbf{l}}$ -texture, coming from the axial anomaly [12]. The anomaly parameter C_0 at $T = 0$ is the same as in Eq. (28).

(3) Finally the third term is the relevant part of the energy of $\hat{\mathbf{l}}$ -texture. There are two other terms in the textural energy [43], containing $(\hat{\mathbf{l}} \cdot (\nabla \times \hat{\mathbf{l}}))^2$ and $(\nabla \cdot \hat{\mathbf{l}})^2$, but they are not important for the stability problem:

The instability starts when the z -dependent disturbances begin to grow. Therefore we are interested only in z -dependent $\hat{\mathbf{l}}$ -textures, which in a quadratic approximation contribute the term $(\hat{\mathbf{l}} \times (\nabla \times \hat{\mathbf{l}}))^2$. The rigidity K_b at low T is logarithmically divergent

$$K_b = \frac{p_F^2 v_F}{24\pi^2 \hbar} \ln \left(\frac{\Delta_0^2}{T^2} \right), \quad (37)$$

which we shall later relate to the zero charge effect in relativistic theories [12].

There is also a topological connection between $\hat{\mathbf{l}}$ and \mathbf{v}_s , since \mathbf{v}_s in Eq. (24) represents torsion of the dreibein $\hat{\mathbf{e}}_1, \hat{\mathbf{e}}_2, \hat{\mathbf{e}}_3$ field. This leads to a nonlinear connection, the so-called Mermin-Ho relation [43], which in our geometry gives

$$\delta \mathbf{v}_s = \frac{\hbar}{2m_3} \hat{\mathbf{z}} \partial_z \Phi + \frac{\hbar}{4m_3} \delta \hat{\mathbf{l}} \times \partial_z \delta \hat{\mathbf{l}} \quad (38)$$

The three variables, the potential Φ of the flow velocity and the two components $\delta \hat{\mathbf{l}} \perp \hat{\mathbf{l}}_0$ of the unit vector $\hat{\mathbf{l}}$, are just another presentation of 3 rotational degrees of freedom of the dreibein $\hat{\mathbf{e}}_1, \hat{\mathbf{e}}_2, \hat{\mathbf{e}}_3$ (the rotation of vectors $\mathbf{m} = c_\perp \hat{\mathbf{e}}_1$, $\mathbf{n} = c_\perp \hat{\mathbf{e}}_2$ and $\hat{\mathbf{l}}$ in Fig. 2). Whereas $\delta \hat{\mathbf{l}}$ is responsible for the effective vector potential of the (hyper) magnetic field, the variable Φ – the angle of rotation of vectors $\mathbf{m} = c_\perp \hat{\mathbf{e}}_1$ and $\mathbf{n} = c_\perp \hat{\mathbf{e}}_2$ about axis $\hat{\mathbf{l}}$ in Fig. 2 – represents an *axion* field as we shall see later.

Let us expand the energy in terms of small perturbations $\delta \hat{\mathbf{l}}$. Adding terms with time derivatives we obtain the following Lagrangian for Φ and $\delta \hat{\mathbf{l}}$:

$$L = F_0 + L_{\delta \hat{\mathbf{l}}} + L_\Phi. \quad (39)$$

Here F_0 is the initial homogeneous flow energy

$$F_0 = \frac{1}{2} m_3 n_3 \mathbf{w}_0^2 - \frac{m^*}{6m_3} p_F^3 \frac{T^2}{\Delta_0^2} (\mathbf{w}_0 \cdot \hat{\mathbf{l}}_0)^2, \quad (40)$$

and $L_{\delta \hat{\mathbf{l}}}$ is the textural Lagrangian of order $(\delta \hat{\mathbf{l}})^2$:

$$L_{\delta \hat{\mathbf{l}}} = \frac{p_F^2}{24\pi^2 \hbar v_F} \ln \left(\frac{\Delta_0^2}{T^2} \right) \left[v_F^2 (\partial_z \delta \hat{\mathbf{l}})^2 - (\partial_t \delta \hat{\mathbf{l}})^2 \right] \quad (41)$$

$$+ \frac{p_F^3}{2\pi^2} (\hat{\mathbf{l}}_0 \cdot \mathbf{w}_0) (\delta \hat{\mathbf{l}} \cdot \nabla \times \delta \hat{\mathbf{l}}) \quad (42)$$

$$+ \frac{m^*}{6} p_F^3 \frac{T^2}{\Delta_0^2} (\mathbf{w}_0 \cdot \hat{\mathbf{l}}_0)^2 (\delta \hat{\mathbf{l}})^2 \quad (43)$$

The first term, Eq.(41), describes the propagation of textural waves (the so-called orbital waves which play the part of the hyperphoton, see below). The Eq.(43) gives the mass of the hyperphoton. The term in Eq.(42) is the Chern-Simons term in action (see below) which is the consequence of the axial anomaly and thus contains the same factor $\frac{p_F^3}{2\pi^2} = (3/2)C_0$ as in Eq. (22). To obtain this factor from the hydrodynamic action for $^3\text{He-A}$

one should collect all the relevant terms: (i) The factor C_0 comes from Eq. (35). (ii) The factor $n_3/2$ – from Eq.(38). And (iii) the factor $-(n_3 - C_0)/2$ – from the intrinsic angular momentum. Altogether they give $C_0 + n_3/2 - (n_3 - C_0)/2 = (3/2)C_0 = p_F^3/2\pi^2$ in Eq. (42). We do not discuss the problem of intrinsic angular momentum, though it is clearly related to the axial anomaly and spectral flow [44]. Here it is important that the contribution of the intrinsic angular momentum to the hydrodynamic action is [12]

$$\frac{1}{2} (n_3 - C_0) \left(\hat{\mathbf{l}}_0 \cdot (\delta \hat{\mathbf{l}} \times (\partial_t + \mathbf{w} \cdot \nabla) \delta \hat{\mathbf{l}}) \right), \quad (44)$$

and this gives the required factor $-(n_3 - C_0)/2$.

L_Φ is the variation of the Lagrangian for superflow. At low T one has

$$L_\Phi = \frac{\hbar^2}{8m_3} n_3 \left[(\partial_z \Phi)^2 - \frac{1}{s^2} (\partial_t \Phi)^2 \right] \quad (45)$$

$$+ \frac{3\hbar}{4m_3} C_0 \partial_z \Phi (\delta \hat{\mathbf{l}} \cdot \nabla \times \delta \hat{\mathbf{l}}) \quad (46)$$

The first two terms of this Lagrangian, contained in Eq. (45), describe the propagation of sound waves (phonons), and s is the speed of sound. We shall later relate the sound waves to axions, because of their coupling with the density of topological charge in Eq. (46).

Let us now establish all these correspondences step by step.

B. Fermionic charge and Chern-Simons energy

In the presence of counterflow, $\mathbf{w} = \mathbf{v}_s - \mathbf{v}_n$, of the motion of the superfluid component of $^3\text{He-A}$ with respect to the normal fraction, the energy of quasiparticles is Doppler shifted by an amount $\mathbf{p} \cdot \mathbf{w}$, which is $\approx \pm p_F (\hat{\mathbf{l}}_0 \cdot \mathbf{w}_0)$ near the nodes. The counterflow therefore produces an effective chemical potential for the relativistic fermions in the vicinity of both nodes (Fig. 8):

$$\mu_R = -p_F (\hat{\mathbf{l}}_0 \cdot \mathbf{w}_0), \quad \mu_L = -\mu_R. \quad (47)$$

According to our analogy the relevant fermionic charge of our system, which is anomalously conserved and which corresponds to the number of right fermions, is the momentum of quasiparticles along $\hat{\mathbf{l}}$ divided by p_F . Since the momentum density of quasiparticles is $\mathbf{P} = -n_{n\parallel} \mathbf{w}$, the density of the fermionic charge is

$$\frac{P}{p_F} = -\frac{n_{n\parallel}}{p_F} \hat{\mathbf{l}}_0 \cdot \mathbf{w}_0. \quad (48)$$

Using Eq. (36) for $n_{n\parallel}$, Eq. (6) and Eq.(4) for the metric tensor, and Eq. (47) for the chemical potential, one obtains a very simple covariant expression for the density of the fermionic charge

Counterflow vs chemical potential for chiral fermions

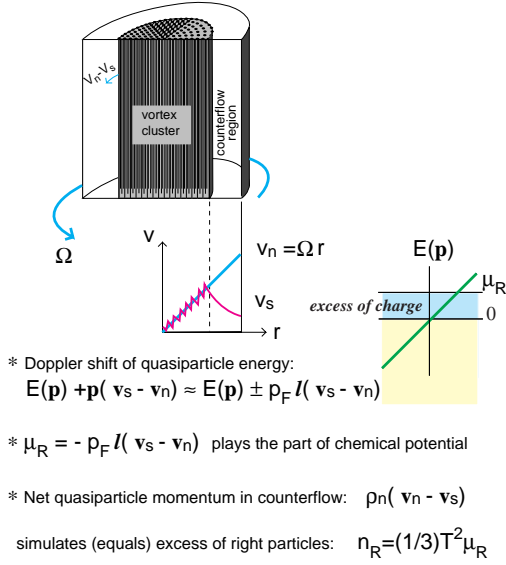


FIG. 8. The counterflow generated by the rotation of the cryostat is equivalent to the nonzero chemical potential for the right electrons. If the cryostat rotates, the typical situation is that the vortices form a vortex cluster in the center of the vessel. Within the cluster the average superfluid velocity $\langle \mathbf{v}_s \rangle$ follows the solid body-like rotation velocity of the normal component: $\langle \mathbf{v}_s \rangle = \mathbf{v}_n = \boldsymbol{\Omega} \times \mathbf{r}$. Outside the cluster the normal component performs a solid body rotation, while the superfluid is irrotational. There results a counterflow $\mathbf{w} = \mathbf{v}_s - \mathbf{v}_n$ between the superfluid and normal components. In the counterflow region the $\hat{\mathbf{l}}_0$ -vector is oriented along the counterflow. The Doppler shift of the quasiparticle energy plays the part of the chemical potential μ_R and μ_L for the chiral fermions in the vicinity of two gap nodes. In the counterflow the quasiparticles have net linear momentum. This excess of the fermionic charge of quasiparticles is equivalent to the excess of chiral right-handed electrons if their chemical potential μ_R is nonzero.

$$n_R \equiv \frac{P}{p_F} = \frac{1}{3} T^2 \mu_R \sqrt{-g}. \quad (49)$$

Here g is the determinant of the metric tensor $g_{\mu\nu}$

$$\sqrt{-g} = \frac{1}{c_{\parallel} c_{\perp}^2} = \frac{m^* p_F}{\Delta_0^2}. \quad (50)$$

Eq. (49) represents the number density of chiral right-handed massless electrons induced by the chemical potential μ_R at temperature T . This is the starting point of the Joyce-Shaposhnikov scenario of magnetogenesis. It is assumed there that at an early stage of the universe, possibly at the Grand Unification epoch (10^{-35} s after the big bang), an excess of chiral right-handed electrons, e_R , is somehow produced due to parity violation.

The equilibrium relativistic energy of the system of right electrons also appears to be completely equivalent to the kinetic energy of the quasiparticles in the counterflow in Eq. (40)

$$\epsilon_R = \frac{1}{6} T^2 \mu_R^2 \sqrt{-g} \equiv \frac{1}{2} m_3 n_{n\parallel} (\mathbf{w}_0 \cdot \hat{\mathbf{l}}_0)^2, \quad (51)$$

The difference in the sign between Eqs. (40) and (51) is the usual difference between the thermodynamic potentials at fixed chemical potential and at fixed particle number (fixed velocity and fixed momentum correspondingly).

Due to the “inverse” axial anomaly the leptonic charge (excess of right electrons) can be transferred to the “inhomogeneity” of the vacuum. This inhomogeneity, which absorbs the fermionic charge, arises as a hypermagnetic field configuration. Thus the charge absorbed by the hypermagnetic field, $\nabla \times \mathbf{A}$, can be expressed in terms of its helicity,

$$n_R \{ \mathbf{A} \} = \frac{1}{2\pi^2} \mathbf{A} \cdot (\nabla \times \mathbf{A}). \quad (52)$$

The right-hand side is the so called Chern-Simons (or topological) charge of the magnetic field.

When this charge is transformed from the fermions to the hypermagnetic field, the energy stored in the fermionic system decreases. This leads to a energy gain which is equal to the Chern-Simons charge multiplied by the chemical potential:

$$F_{CS} = n_R \{ \mathbf{A} \} \mu_R = \frac{1}{2\pi^2} \mu_R \mathbf{A} \cdot (\nabla \times \mathbf{A}). \quad (53)$$

The translation to the language of $^3\text{He-A}$, according to the dictionary in Fig. (9), gives the following energy change, if the texture is formed from the counterflow,

$$F_{CS} = \frac{p_F^3}{2\pi^2} (\hat{\mathbf{l}}_0 \cdot \mathbf{w}_0) (\delta \hat{\mathbf{l}} \cdot \nabla \times \delta \hat{\mathbf{l}}). \quad (54)$$

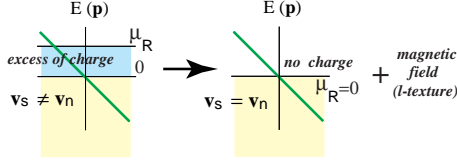
This exactly coincides with Eq. (42).

The Chern-Simons term in Eqs. (53,54) can have arbitrary sign. It is positive if the counterflow is increased and negative if the counterflow is reduced. Thus one can have an energy gain from the transformation of the counterflow (fermionic charge) to the texture (hypermagnetic field). This energy gain is however to be compared with the positive energy terms in Eq. (41) and Eq. (43). Let us consider these two terms in more detail.

C. Maxwell Lagrangian for hypermagnetic and hyperelectric fields.

The Lagrangian for the $\delta \hat{\mathbf{l}}$ -texture in Eq. (41) is completely equivalent to the conventional Maxwell Lagrangian for the (hyper-) magnetic and electric fields. For

Flow instability
vs
instability of state with excess of chiral charge



Dictionary

Particle physics	${}^3\text{He-A}$
Chern-Simons term leading to helical instability:	
	$(1/2\pi^2)\mu_R \mathbf{A}(\nabla \times \mathbf{A})$
Chemical potential μ_R	$= \rho_F I_0 (v_s - v_n)$
Vector potential \mathbf{A}	$= \rho_F (\mathbf{l} - I_0)$
Magnetic field	$= \text{helical texture}$
$F_{ik} = \nabla_i A_k - \nabla_k A_i$	$= \rho_F (\nabla_i l_k - \nabla_k l_i)$
Magnetic field energy	$= \text{Energy of texture}$
	$(1/12\pi^2) \ln(\Lambda/T) \sqrt{-g} g^{ij} g^{kl} F_{ik} F_{jl}$
Metric tensor g^{ij}	$= c_{ }^2 \hat{l}^i \hat{l}^j + c_{\perp}^2 (\delta^{ij} - \hat{l}^i \hat{l}^j)$
Planck energy Λ	$= \text{gap amplitude } \Delta_0$

FIG. 9. An excess of chiral right-handed electrons in the early Universe can be effectively converted to a hypermagnetic field via the mechanism of chiral anomaly. This is described essentially by the same equations as the counterflow instability observed in ${}^3\text{He-A}$.

example the textural energy, written in covariant form, corresponds to the magnetic energy:

$$F_{\text{magn}} = \ln \left(\frac{\Delta_0^2}{T^2} \right) \frac{p_F^2 v_F}{24\pi^2 \hbar} (\partial_z \delta \hat{\mathbf{l}})^2 \quad (55)$$

$$\equiv \frac{\sqrt{-g}}{2\gamma^2} g^{ij} g^{kl} F_{ik} F_{jl} \quad (56)$$

Here, $F_{ik} = \nabla_i A_k - \nabla_k A_i$, and γ^2 is a running coupling constant, which is logarithmically divergent because of vacuum polarization in a complete analogy with the fine structure constant $e^2/4\pi\hbar c$:

$$\gamma^{-2} = \frac{1}{12\pi^2} \ln \left(\frac{\Delta_0^2}{T^2} \right) \quad (57)$$

Eq. (56) transforms to Eq. (55) if one takes into account that in our geometry the “hypermagnetic” field $\mathbf{B} \perp \hat{\mathbf{l}}_0$.

The gap amplitude Δ_0 , constituting the ultraviolet cut-off in the logarithmically divergent magnetic energy, plays the part of the Planck energy scale. Note that Δ_0 has a parallel with the Planck energy in some other situations, too. For example the analogue of the cosmological constant, which arises in the effective gravity of ${}^3\text{He-A}$, has the value $\Delta_0^4/12\pi^2$ [45].

D. Mass of hyperphoton

The “hyperphoton” in ${}^3\text{He-A}$ has a mass. There are several sources of this mass.

(i) The value of the mass of the “hyperphoton” is seen from Eq. (43), if it is written in covariant form:

$$F_{\text{mass}}(T, \mu_R) = \frac{1}{6} \sqrt{-g} g^{ik} A_i A_k \frac{T^2 \mu_R^2}{\Delta_0^2} \quad (58)$$

Thus the mass is

$$M_{ph}^2 = \frac{\gamma^2}{3} \frac{T^2 \mu_R^2}{\Delta_0^2} \quad (59)$$

In ${}^3\text{He-A}$ this mass is physical, though it contains the “Planck” energy cut-off Δ_0 : The “hyperphoton mass” is the gap in the spectrum of orbital waves, propagating oscillations of $\delta \hat{\mathbf{l}}$, which correspond just to the hyperphoton. This mass appears due to the presence of counterflow, which provides the restoring force for oscillations of $\delta \hat{\mathbf{l}}$.

For the relativistic counterpart of ${}^3\text{He-A}$, the Eq. (59) suggests that the mass of the hyperphoton could arise if both the temperature T and the chemical potential μ_R are finite. Of course, in the case of exact local $U(1)$ symmetry, the mass of the hyperphoton should be zero. But in an effective theory, the local $U(1)$ symmetry appears only in the low-energy corner and thus is approximate. It can be violated (not spontaneously) at higher energy leading to a nonzero hyperphoton mass which depends on the cut-off parameter. And in fact the mass in Eq. (59) disappears in the limit of an infinite cut-off parameter or is small, if the cut-off is of Planck scale. The ${}^3\text{He-A}$ thus provides an illustration of how the terms of order $(T/E_{\text{Planck}})^2$ appear in the effective quantum field theory [46].

(ii) In the collisionless regime $\omega\tau \gg 1$, a nonzero mass term is present even in the absence of the counterflow, $\mathbf{w} = 0$. It corresponds to the high-frequency photon mass in the relativistic plasma, calculated by Weldon [47]:

$$M_{ph}^2(\omega\tau \gg 1) = \frac{N_F}{18} \gamma^2 T^2 \quad (60)$$

Here N_F is the number of fermionic species and γ again is the running coupling constant. This can be easily translated to ${}^3\text{He-A}$ language, since mass is a covariant quantity. Substituting the running coupling from Eq. (57) and taking into account that the number of the fermionic species in ${}^3\text{He-A}$ is $N_F = N_{FR} + N_{FL} = 2$, one obtains the gap in the spectrum of the high-frequency orbital waves (called also the normal flapping mode)

$$M_{\text{orb waves}}^2(\omega\tau \gg 1) = \frac{4\pi^2}{3} \frac{T^2}{\ln(\Delta_0^2/T^2)} \quad (61)$$

This coincides with Eq. (11.76b) of Ref. [43] for the normal flapping mode. Note that in ${}^3\text{He-A}$ this gap in the

spectrum, corresponding to the relativistic plasma oscillations, was obtained by Wölfle already in 1975 [48].

The corresponding mass term in the Lagrangian for the gauge bosons is

$$F_{mass}(T, \omega\tau \gg 1) = \frac{N_F}{36} T^2 \sqrt{-g} g^{ik} A_i A_k . \quad (62)$$

which is valid both for the proper relativistic theory with chiral fermions and for ${}^3\text{He-A}$, where $N_F = 2$.

(iii) There is also the topological mass of the “photon” in ${}^3\text{He-A}$, which comes from the axial anomaly and intrinsic angular momentum [12,49,50]. It is rather small.

(iv) The tiny mass coming from the spin-orbital interaction in ${}^3\text{He-A}$ [50] is described by the energy term [43]

$$-g_D(\hat{\mathbf{l}} \cdot \hat{\mathbf{d}})^2 , \quad (63)$$

where $\hat{\mathbf{d}}$ is the unit vector of the spontaneous anisotropy in spin space. This term has no counterpart in relativistic theories but is important in NMR experiments on ${}^3\text{He-A}$ (see below).

Here we discussed how the “photon” mass in ${}^3\text{He-A}$ is influenced by various external and internal factors: counterflow (chemical potential), temperature, anomaly, spin-orbital interaction, Planck cut-off parameter. These factors also influence the speed of “light” in ${}^3\text{He-A}$ and this occurs essentially in the same manner as in relativistic theories (see [51] for references on the modification of the speed of light by electromagnetic fields, temperature, gravitational background, and other external environments). The only difference is that in ${}^3\text{He-A}$ the environment modifies the Planck cut-off parameter as well [52], which gives an extra dependence of the “photon” mass and the speed of “light” on the environment.

E. Instability towards magnetogenesis

For us the most important property of the axial anomaly term in Eqs. (53,54) is that it is linear in the derivatives of $\delta\hat{\mathbf{l}}$. Its sign thus can be negative, while its magnitude can exceed the positive quadratic term in eq. (55). This leads to the helical instability towards formation of the inhomogeneous $\delta\hat{\mathbf{l}}$ -field. During this instability the kinetic energy of the quasiparticles in the counterflow (analogue of the energy stored in the fermionic degrees of freedom) is converted into the energy of the inhomogeneity $\nabla_z \delta\hat{\mathbf{l}}$, which is the analogue of the magnetic energy of the hypercharge field.

This instability can be found by investigation of the eigenvalues of the quadratic form describing the energy in terms of $\mathbf{A} = p_F \delta\hat{\mathbf{l}}$ in Eq.(41-43). Using the covariant form of this equation one obtains the following 2×2 matrix for two components of the vector potential, $A_x = A_{x0} e^{iqz}$ and $A_y = A_{y0} e^{iqz}$:

$$\begin{pmatrix} M_{ph}^2 + c_{\parallel}^2 q^2 & \frac{\gamma^2}{2\pi^2} \mu_R c_{\parallel} q \\ \frac{\gamma^2}{2\pi^2} \mu_R c_{\parallel} q & M_{ph}^2 + c_{\parallel}^2 q^2 \end{pmatrix} . \quad (64)$$

This matrix is applied both to the Joyce-Shaposhnikov scenario and to the instability of the ${}^3\text{He-A}$ superflow. This is one of the rare cases when the equation of motion for the $\hat{\mathbf{l}}$ -vector reduces to relativistic (Maxwell + Chern-Simons) equations. This stems from the fact that for the investigation of the stability one needs an energy which is quadratic in terms of the small deviations of the vector potential (vector $\hat{\mathbf{l}}$) from the uniform background. In our geometry: (i) The equilibrium unit vector $\hat{\mathbf{l}}_0$ is oriented in one direction (along the velocity), which means that the background metric is constant in space. (ii) Small deviations $\delta\hat{\mathbf{l}} \equiv \mathbf{A}/p_F$ of the vector $\hat{\mathbf{l}}$ from equilibrium are perpendicular to the flow, while the relevant coordinate dependence (i.e. that which leads to instability) is the z -dependence along the flow. Thus there are no derivatives in x and y in the relevant Lagrangian, while \mathbf{A} contains only the transverse components. (iii) The Lagrangian is quadratic in the gauge field $\mathbf{A} \equiv p_F \delta\hat{\mathbf{l}}$, while the metric enters only as a constant (though anisotropic) background. All these facts conspire to produce a complete analogy with the relativistic theory. Such a geometry, in which the analogy is exact, is really unique, and it might be called a miracle that it indeed does occur in a real experimental situation.

The quadratic form in Eq. (64) becomes negative if

$$\frac{\mu_R}{M_{ph}} > \frac{4\pi^2}{\gamma^2} . \quad (65)$$

Inserting the photon mass from Eq. (59), one finds that the uniform counterflow becomes unstable towards the nucleation of the texture if

$$\frac{T}{\Delta_0} \ln^{1/2} \left(\frac{\Delta_0^2}{T^2} \right) < \frac{3}{2\pi} . \quad (66)$$

If this condition is fulfilled, the instability occurs for any value of the counterflow (any value of the chemical potential μ_R of right electrons).

In relativistic theories, where Δ_0 is the Planck energy, this condition is always fulfilled. Thus the excess of the fermionic charge is always unstable towards nucleation of the hypermagnetic field. In the scenario of the magnetogenesis developed by Joyce and Shaposhnikov [39,40], this instability is responsible for the genesis of the hypermagnetic field well above the electroweak transition. The role of the subsequent electroweak transition is to transform this hypermagnetic field to the conventional (electromagnetic $U(1)$) magnetic field due to the electroweak symmetry breaking.

In ${}^3\text{He-A}$ the instability occurs only if the temperature is low enough compared to Δ_0 ($\Delta_0 \sim 2T_c$ [43]). In our analysis we used the limit $T \ll \Delta_0$, which is why

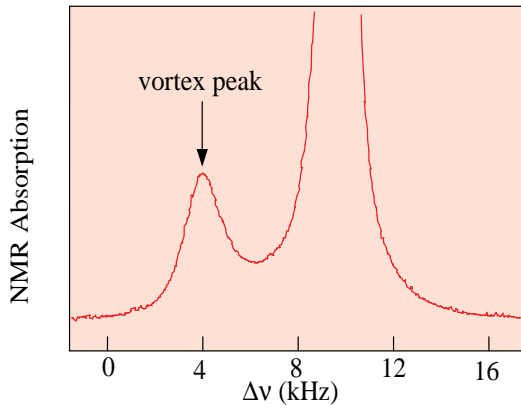


FIG. 10. The NMR signal from array of ATC vortices in the container. The position of the satellite peak indicates the type of the vortex, while the intensity is proportional to the number of vortices of this type in the cell.

the condition (66) is only very approximate. The helical instability in $^3\text{He-A}$ has been intensively discussed theoretically (see, e.g., [53]). According to a rigorous theory, which holds at any T and gives the result, depending on Fermi-liquid parameters, the counterflow becomes unstable at T below about $0.8T_c$ (see Sec. 7.10.1 in the book [43]). The result of the helical instability can be either the formation of the helical texture with small opening angle or the complete collapse of the counterflow. In the first case only some part of the counterflow momentum transforms to the momentum of the helix. In the second case the collapse of the counterflow leads to the formation of continuous ATC vortices and thus the whole counterflow momentum is transformed to the momentum carried by the vortex texture. Experimentally the second scenario, with formation of vortices, is realized [42].

F. “Magnetogenesis” in $^3\text{He-A}$

In various experiments [42,54,41] the flow instability has been measured using NMR techniques, which means that one needs an external (real) magnetic field \mathbf{H} . Such a field adds an additional mass to the “hypercharge gauge field” \mathbf{A} due to the spin-orbital interaction in Eq. (63). Even at low T the instability then occurs only above some critical value of the counterflow velocity w_0 (or correspondingly chemical potential of right electrons μ_R). The critical value μ_R^{cr} depends on T and H .

When this helical instability develops in $^3\text{He-A}$, the final result is the formation of the $\hat{\mathbf{l}}$ -texture which corresponds to the free energy minimum in the rotating vessel. This is the periodic $\hat{\mathbf{l}}$ -texture, whose elementary cell represents the Anderson-Toulouse-Chechetkin (ATC) continuous vortex in Fig. 5. The presence of ATC vortices and their number is extracted from the NMR absorp-

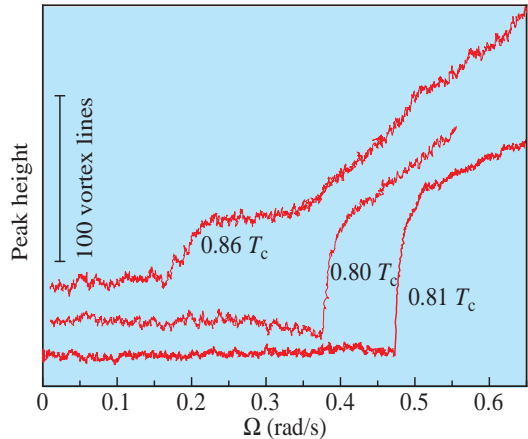


FIG. 11. Time dependence of the satellite peak height of the continuous vortices. Initially vortices are not present in the vessel. When the velocity of the counterflow \mathbf{w} in the $\hat{\mathbf{l}}_0$ direction (corresponding to the chemical potential μ_R of the chiral electrons) exceeds some critical value, the instability occurs and the container becomes filled with the $\hat{\mathbf{l}}$ -texture (hypermagnetic field) forming the vortex array.

tion spectrum, which contains the satellite peaks coming from different types of vortices [55]. The position of the satellite peak indicates the type of vortex, while the intensity is proportional to the number of vortices of this type. The satellite peak for the ATC vortices is shown in Fig. 10.

In the experiment carried out in Helsinki the initial state did not contain vortices. Then the vessel was put into rotation with some angular velocity Ω . If the velocity is small enough, one has only counterflow and no vortex texture. This means that there is a nonzero “chemical potential of right electrons”, $\mu_R = p_F \Omega r$, where r is the distance from the axis of the rotating vessel, while the “hypermagnetic” field is absent. Accelerating the vessel further one finally reaches the critical value μ_R^{cr} at the wall of container, $r = R$, where the counterflow is maximal. At this moment the instability occurs, which is observed by the Helsinki group as a jump in the height of the vortex peak (see Fig. 11). The peak height jumps from zero to the magnitude corresponding to a vortex array with nearly the equilibrium number of vortex lines. This means that counterflow has been essentially removed. The counterflow (which carried the fermionic charge of matter) has thus been converted to a vortex $\hat{\mathbf{l}}$ -texture (hypermagnetic field).

The magnitude of μ_R^{cr} found from experiments [42] was in good quantitative agreement with the theoretical estimation of the mass of the “hyperphoton” determined by the spin-orbit interaction in Eq. (63). Thus the Helsinki experiments model the nucleation of the hypermagnetic field for different masses of the “hyperphoton”. The flow instability in the limit when the contribution to the “hy-

perphoton” mass from the real external magnetic field H is zero has also been investigated: First the field H was turned off and after the instability had occurred the field was switched on again and the created “hypermagnetic field” was measured. In this case it was observed that μ_R^{cr} was significantly reduced.

V. AXION IN ${}^3\text{He-A}$

We discussed how the quasiparticles and the $\hat{\mathbf{l}}$ -texture can exchange the fermionic charge – the linear momentum – due to the axial anomaly. There is yet another phenomenon: The $\hat{\mathbf{l}}$ -texture and the moving superfluid vacuum can also exchange momentum. Thus the $\hat{\mathbf{l}}$ -texture serves as an intermediate object which allows to transfer the fermionic charge from the condensate (vacuum) motion to the quasiparticles (matter), as was discussed in Sec.IIIA. In this sense the $\hat{\mathbf{l}}$ -texture plays the same role as quantized vortices in superfluids and superconductors. This again shows the common properties of continuous $\hat{\mathbf{l}}$ -textures (with continuous vorticity) and quantized singular vortices, which are related to the gap nodes: In the $\hat{\mathbf{l}}$ -textures the gap nodes are lying in momentum space, while in the most symmetric quantized vortices of conventional superconductors and also in the most symmetric cosmic strings the nodes are in real space – in the cores of vortices, where the symmetry is restored and fermions are massless. The transformation between the real-space zeroes and the momentum-space zeros [56] actually occurs when the singular core of the vortex experiences an additional symmetry breaking, as was observed for the ${}^3\text{He-B}$ vortices. The relation of both types of zeroes to the axial anomaly was discussed in [57].

Consider now the exchange between the superfluid vacuum and the texture. The momentum density of the superfluid vacuum along the equilibrium $\hat{\mathbf{l}}_0$ -vector is $m_3 n_3 v_{sz}$. The momentum exchange follows from the anomalous nonconservation of the momentum Eq. (22):

$$m_3 n_3 (\partial_t v_{sz} + \partial_z \mu_3) = \frac{p_F}{2\pi^2} (\partial_t \mathbf{A} \cdot \nabla \times \mathbf{A}) . \quad (67)$$

where μ_3 is the real chemical potential of ${}^3\text{He}$ atoms, which also determines the speed of sound in ${}^3\text{He-A}$: $s^2 = n_3 d\mu_3 / dn_3$; $\mathbf{A} = p_F \delta \hat{\mathbf{l}}$. In what follows, we consider only the z - and t -dependence of all variables.

Let’s introduce a variable θ which is dual to the potential Φ of the superflow:

$$\partial_t \theta = -\frac{p_F}{2m_3} \partial_z \Phi = -p_F v_{sz} , \quad (68)$$

$$\partial_z \theta = -\frac{p_F}{2m_3 s^2} \partial_t \Phi = \frac{p_F}{s^2} \delta \mu_3 , \quad (69)$$

We can now write down the Lagrangian whose variation gives rise to the anomalous nonconservation of the condensate momentum in Eq. (67):

$$\frac{1}{2\pi^2} \theta \left(\partial_t \vec{A} \cdot \vec{\nabla} \times \vec{A} \right) + \frac{n_3 m_3}{2p_F^2} (s^2 (\partial_z \theta)^2 - (\partial_t \theta)^2) . \quad (70)$$

This is nothing but the action for the axion field θ , which interacts with the CP violating combination $F^{\mu\nu} \hat{F}_{\mu\nu} \propto \mathbf{E} \cdot \mathbf{B}$ [58].

In ${}^3\text{He-A}$ the axion corresponds to sound waves – propagating oscillations of two conjugated variables, the phase Φ , related to rotations of the fundamental triad, and the particle density n_3 . The anomalous first term in Eq. (70) can be also obtained from Eq. (46). The speed of sound is $s^2 = (1/3)v_F^2(1+F_0)(1+F_1/3)$, where F_0 and F_1 are Fermi-liquid parameters, and is the same in superfluid ${}^3\text{He-A}$ ($T < T_c$) and in normal liquid ${}^3\text{He}$ ($T > T_c$). In distinction from the orbital waves (“electromagnetic waves”), the speed of sound s is isotropic and does not coincide with any of the two speeds of light, c_\perp or c_\parallel , though one can expect that the axion propagating along z must have the parallel speed of “light” $c_\parallel = v_F$. What is the reason? It is a property of the superfluid ${}^3\text{He-A}$:

Both modes, “photon” (orbital wave) and “axion” (sound wave) are collective bosonic excitations of the fermionic system and are obtained by integration over the fermions. In the case of “photons” the relevant region of the integration over the fermions is concentrated close to the gap nodes due to the logarithmic divergency. Near the nodes the fermions are relativistic and are described by the Lorentzian metric $g^{\mu\nu}$. It follows that the effective “photons” are described by the same metric and therefore the speed of light is the same as the speed of the massless fermion propagating in the same direction. On the other hand, the relevant region of the integration, which is responsible for the spectrum of the “axion” mode, is far from the gap nodes. Consequently the axion spectrum does not even depend on the existence of the gap nodes and induces its own effective metric.

VI. DISCUSSION

In principle one can introduce a model system with favourable parameters, such that for all collective modes the integration over the fermions is concentrated mostly in the region where the fermions are Lorentzian. In this case the low energy dynamics of photons, axions, gravitons, etc., will be determined by the same Lorentzian metric as that of the fermions. In the low-energy corner, one then obtains the effective relativistic quantum field theory and effective quantum gravity with the same speed of light for all bosons and fermions.

It is quite possible that in this ideal case the cosmological constant vanishes. This follows from the fact that Eq. (3) for the spectrum of massless quasiparticles can be multiplied by an arbitrary scaling factor a^2 , which does not change the energy spectrum, but changes the contravariant metric tensor: $g^{\mu\nu} \rightarrow a^2 g^{\mu\nu}$. Since

physics cannot depend on such formal conformal transformation, the effective low-energy Lagrangian for gravity cannot depend on a^2 and thus the cosmological term $\int d^3x dt \Lambda \sqrt{-g}$ is prohibited (a discussion of the role of the scale invariance for vanishing cosmological constant is found in Ref. [59]).

This situation is somewhat similar to that which occurs in the normal Fermi-liquid where the role of the parameter a^{-1} is played by the quasiparticle spectral weight Z – the residue of the Green’s function at the quasiparticle pole. The low-energy properties of this system, described by the Landau phenomenological Fermi-liquid theory, do not depend on Z . The Landau Fermi-liquid differs from our system only in the topology of the spectrum of the low-lying fermionic excitations: The Fermi-surface instead of the Fermi-points – the gap nodes, is present there.

Note that the Fermi-surface and the point node are the only topologically stable features of the fermionic spectrum. They are described by π_1 and π_3 topological invariants respectively and thus are robust to any modification of the system. These two classes exhaust the topologically stable gapless Fermi systems. In Landau theory, which deals with the Fermi-surface class of Fermi liquids, the low-energy bosonic collective modes are related to the dynamical deformations of the Fermi surface. In the point-node class of Fermi liquids, the corresponding collective motion comes from the dynamics of the nodes. This dynamics gives rise to effective gravity and effective electromagnetic fields.

The fundamental constants in these effective theories are determined by the position of the node, p_F , and by the slopes of the energy E of the quasiparticle as a function of its momentum \mathbf{p} at the node. There are three such parameters in $^3\text{He-A}$: the Fermi velocity v_F , the Fermi momentum p_F and the gap amplitude Δ_0 . They give the parallel speed of light $c_{\parallel} = v_F$; the transverse speed of light $c_{\perp} = \Delta_0/p_F$; the Planck energy Δ_0 ; the running coupling constant in Eq. (57); the masses of the hyperphoton in Eqs. (59,60); gravitational constant $G \sim \Delta_0^{-2}$ [52] and cosmological constant $\sim \Delta_0^4$ [45]; etc. Since all 3 initial parameters are in principle temperature dependent, the fundamental constants are not constants in the effective theories. For example the speed of light depends on temperature and also on the photon energy: $\delta c/c \sim (E/E_{\text{Planck}})^2$.

We discussed only 3 experiments in superfluid $^3\text{He-A}$ related to the properties of the electroweak vacuum. In all of them the chiral anomaly is an important mechanism. It regulates the nucleation of the fermionic charge from the vacuum, as observed in Manchester [28], and the inverse process of the nucleation of the effective magnetic field from the fermion current, as observed in Helsinki [42,41].

There are many other connections between superfluid ^3He and different branches of physics which should be

explored. For example, we can simulate phenomena related to the effective gravity, such as the cosmological constant, quantum properties of the event horizon, vacuum instability in strong gravity, torsion strings and even inflation. In principle a nonequilibrium vacuum state can be constructed in which the speed of light $c_{\perp} = \Delta_0/p_F$ decreases exponentially with time. In cosmological language this implies inflation, since the length scale in the spatial metric g_{ik} is growing exponentially. This would allow for a study of the development of perturbations during inflation.

Till now we considered the properities related to one pair of nodes only. If one takes into account that in $^3\text{He-A}$ there is a two-fold degeneracy related to two spin projection of the ^3He atom, the number of fermionic and bosonic degrees of freedom increases. It appears that with these new degrees of freedom, the system transforms to a $SU(2)$ gauge theory: The conventional spin degrees of freedom of ^3He atoms form the $SU(2)$ isospin, while some collective modes of the order parameter (the spin-orbital waves) behave as $SU(2)$ gauge bosons [12].

There are several ways of extending the model, in which higher local and global symmetry groups can naturally arise. (1) One can imagine an initial normal state of condensed matter consisting of $n = 3, 4$, etc. degenerate sheets of the Fermi-surface. Then the superconducting/superfluid Cooper pairing will lead to n -fold degeneracy of gap nodes, which in turn gives rise to the effective local $SU(n)$ group in the low-energy corner. (2) The number of gap nodes on each Fermi-surface can be also larger than 2. For example the so called α -state of ^3He [43] contains 8 gap nodes per Fermi-surface and thus 8 elementary relativistic fermions in the vicinity of the nodes. The fluctuations of positions of these nodes are equivalent to several gauge fields. In high- T_c superconductivity each Fermi-sheet (actually the Fermi-circle since this kind of superconductivity effectively occurs in the two-dimensional space of the CuO plane) contains 4 gap nodes. The corresponding Weyl-like Hamiltonian for 4 fermions and the corresponding gauge fields have been discussed for this material in Ref. [60]. Thus in principle it appears possible to construct a model which has as many fermionic and bosonic degrees of freedom as needed in Grand Unified Theories, including the different generations of fermions. Of course, the construction of a suitable condensed matter system corresponding to such a model is not a simple undertaking.

VII. ACKNOWLEDGEMENTS

I thank Uwe Fischer, Henry Hall, John Hook, Ted Jacobson, Michael Joyce, Tom Kibble, Matti Krusius, Robert Laughlin, Misha Shaposhnikov, Alexei Starobinsky, Tanmay Vachaspati and Shuqian Ying for fruitful discussions.

-
- [1] F. Wilczek, “The Future of Particle Physics as a Natural Science”, hep-ph/9702371.
- [2] H.B. Nielsen, “Field theories without fundamental (gauge) symmetries”, preprint NBI-HE-83-41.
- [3] A.D. Sakharov, Sov. Phys. Doklady **12**, 1040 (1968).
- [4] Ya.B. Zeldovich, “Interpretation of electrodynamics as a consequence of quantum theory”, Pis'ma ZhETF **6**, 922 (1967) [JETP Lett. **6** 345 (1967)].
- [5] R. Laughlin, “Gauge Theories from Nothing in Condensed Matter: Are Quantum Critical Points Supersymmetric Field Theories”, talk at the Symposium on QUANTUM PHENOMENA at LOW TEMPERATURES, Lammi, 7-11 January, 1998; see also “Parallels Between Quantum Antiferromagnetism and the Strong Interactions”, Proceedings of the Inauguration Conference of the Asia-Pacific Center for Theoretical Physics, Seoul National University, Korea 4-10 June 1996, ed. by Y. M. Cho, J. B. Hong, and C. N. Yang (World Sci., Singapore, 1998), cond-mat/9802180.
- [6] G.E. Volovik, “Simulation of Quantum Field Theory and Gravity in Superfluid He-3”, cond-mat/9706172.
- [7] T. Jacobson and G.E. Volovik, “Event horizons and ergoregions in ^3He ”, cond-mat/9801308.
- [8] N. B. Kopnin and G. E. Volovik, “Rotating vortex core: An instrument for detecting the core excitations”, Phys. Rev. **B 57** 8526 (1998).
- [9] W.G. Unruh, “Experimental black-hole evaporation?”, Phys. Rev. Lett. **46** 1351 (1981); “Sonic analogue of black holes and the effects of high frequencies on black hole evaporation,” Phys. Rev. **D 51** 2827 (1995).
- [10] T. Jacobson, “Black hole evaporation and ultrashort distances”, Phys. Rev. **D 44** 1731 (1991).
- [11] M. Visser, “Acoustic black holes: horizons, ergospheres, and Hawking radiation”, gr-qc/9712010.
- [12] G.E. Volovik, Exotic properties of superfluid ^3He , World Scientific, Singapore-New Jersey-London-Hong Kong, 1992.
- [13] G.E. Volovik and T. Vachaspati, “Aspects of ^3He and the standard electroweak model”, Int. J. Mod. Phys. **B 10**, 471 (1996).
- [14] S.H. Simon and P.A. Lee, “Scaling of the quasiparticle spectrum for d -wave superconductors”, Phys. Rev. Lett., **78**, 1548 (1997); **78**, 5029 (1997).
- [15] X.G. Wen, Phys. Rev. B, **43**, 11025 (1991).
- [16] M. Stone, Annals of Phys., **207**, 38 (1991).
- [17] R.B. Laughlin, “Magnetic Induction of $d + i d$ Order in High-Tc Superconductors”, cond-mat/9709004.
- [18] G.E. Volovik, “On edge states in superconductor with time inversion symmetry breaking”, JETP Lett. **66**, 522 (1997).
- [19] S. Ying, “The Quantum Aspects of Relativistic Fermion Systems with Particle Condensation”, hep-th/9711167; M. Alford, K. Rajagopal, F. Wilczek, “QCD at Finite Baryon Density: Nucleon Droplets and Color Superconductivity”, hep-ph/9711395.
- [20] K. Kajantie, M. Laine, K. Rummukainen, and M. Shaposhnikov, “Is there a hot electroweak transition at $m_H \geq m_W$?”, Phys. Rev. Lett. **77**, 2887 (1996), see also discussion in A. Rajantie, “Vortices and the Ginzburg-Landau phase transition”, Proceedings of the Symposium on QUANTUM PHENOMENA at LOW TEMPERATURES, Lammi, 7-11 January, 1998 (this volume).
- [21] S. Adler, “Axial-vector vertex in spinor electrodynamics”, Phys. Rev. **177**, 2426 (1969).
- [22] J.S. Bell and R. Jackiw, “A PCAC puzzle: $\pi^0 \rightarrow \gamma\gamma$ in the σ -model”, Nuovo Cim. **A60**, 47–61 (1969).
- [23] V.R. Chechetkin, JETP, **44**, 706 (1976).
- [24] P.W. Anderson and G. Toulouse, Phys. Rev. Lett., **38**, 508 (1977).
- [25] G.E. Volovik, “Hydrodynamic action for orbital and superfluid dynamics of $^3\text{He-A}$ at $T = 0$ ”, JETP **75**, 990 (1992).
- [26] G.E. Volovik, “Three nondissipative forces on a moving vortex line in superfluids and superconductors”, JETP Lett. **62**, 65 (1995); “Vortex vs spinning string: Jordan-kii force and gravitational Aharonov-Bohm effect”.
- [27] N.B. Kopnin, “Mutual friction in superfluid ^3He . II. Continuous vortices in $^3\text{He-A}$ at low temperatures”, Phys. Rev. **B 47**, 14354 (1993).
- [28] T.D.C. Bevan, A.J. Manninen, J.B. Cook, J.R. Hook, H.E. Hall, T. Vachaspati and G.E. Volovik, “Momentumgenesis by ^3He vortices: an experimental analogue of primordial baryogenesis”, Nature, **386**, 689 (1997).
- [29] T.D.C. Bevan, A.J. Manninen, J.B. Cook, H. Alles, J.R. Hook, H.E. Hall, “Vortex mutual friction in superfluid ^3He vortices”, J. Low Temp. Phys. **109**, 423 (1997).
- [30] A.D. Dolgov, “Non-GUT baryogenesis”, Rep. Prog. Phys., **222**, 309 (1992).
- [31] N. Turok, in “Formation and interaction of topological defects”, eds. A.C. Davis, R. Brandenberger (Plenum Press, New York, London), 1995, pp. 283–301.
- [32] E. Witten, Nucl. Phys. **B249**, 557 (1985).
- [33] T. Vachaspati and G.B. Field, “Electroweak string configurations with baryon number”, Phys. Rev. Lett. **73**, 373–376 (1994); **74**, 1258(E) (1995).
- [34] J. Garriga and T. Vachaspati, “Zero modes on linked strings”, Nucl. Phys. **B 438**, 161 (1995).
- [35] M. Barriola, “Electroweak strings produce baryons”, Phys. Rev. **D 51**, 300 (1995).
- [36] G.D. Starkman and T. Vachaspati, “Galactic cosmic strings as sources of primary antiprotons”, Phys. Rev. **D 53**, 6711 (1996).
- [37] N.B. Kopnin, G.E. Volovik, and Ü. Parts “Spectral flow in vortex dynamics of $^3\text{He-B}$ and superconductors”, Europhys. Lett. **32** 651 (1995).
- [38] M. Stone, “Spectral flow, Magnus force and mutual friction via the geometric optics limit of Andreev reflection”, Phys. Rev. **B 54**, 13222 (1996).
- [39] M. Joyce, M. Shaposhnikov, “Primordial magnetic fields, right electrons, and the abelian anomaly”, Phys. Rev. Lett., **79**, 1193 (1997).
- [40] M. Giovannini and E.M. Shaposhnikov, “Primordial hypermagnetic fields and triangle anomaly”, Phys. Rev. **D 57** 2186 (1998).
- [41] M. Krusius, T. Vachaspati and G.E. Volovik “Flow instability in $^3\text{He-A}$ as analog of generation of hypermagnetic field in early Universe”, cond-mat/9802005.

- [42] V.M.H. Ruutu, J. Kopu, M. Krusius, U. Parts, B. Plaaais, E.V. Thuneberg, and W. Xu , “Critical velocity of vortex nucleation in rotating superfluid $^3\text{He-A}$ ”, Phys. Rev. Lett., **79**, 5058 (1997).
- [43] D. Vollhardt, P. and P. Wölfle, “The superfluid phases of helium 3”, Taylor and Francis, London - New York - Philadelphia, 1990.
- [44] G.E. Volovik, “Orbital momentum of vortices and textures due to spectral flow through the gap nodes: Example of the $^3\text{He-A}$ continuous vortex”, JETP Lett. **61**, 958 (1995).
- [45] G.E. Volovik, “Analog of gravity in superfluid $^3\text{He} - A$ ”, JETP Lett. **44**, 498 (1986).
- [46] F. Jegerlehner, ”The “ether-world and elementary particles”, hep-th/9803021.
- [47] H.A. Weldon, “Covariant calculations at finite temperature: The relativistic plasma”, Phys. Rev. **D 26**, 1394 (1982).
- [48] P. Wölfle, in “Quantum Statistics and the Many Body Problem” (S.B. Trickey, W.P. Kirk, and J.W. Duffy, Eds.) p.9. Plenum, New York, 1975.
- [49] G.E. Volovik, “Orbital momentum and orbital waves in the anisotropic A-phase of superfluid ^3He ”, JETP Lett. **22**, 108 (1975); “Dispersion of the orbital waves in the A-phase of superfluid ^3He ”, JETP Lett. **22**, 198 (1975).
- [50] A.J. Leggett and S. Takagi, “Orientational Dynamics of Superfluid ^3He : A “Two-Fluid” Model. II. Orbital Dynamics”, Ann. Phys. **110**, 353 (1978).
- [51] W. Dittrich, and H. Gies “Light propagation in non-trivial QED vacua”, hep-ph/9804375.
- [52] G.E. Volovik, “Gravity of monopole and string and gravitational constant in $^3\text{He-A}$ ”, cond-mat/9804078.
- [53] D. Vollhardt, “Stability of supeflow and related textural transformations in superfluid ^3He ”, PhD Thesis, Hamburg, 1979.
- [54] V.M.H.Ruutu, V.B.Eltsov, A.J.Gill, T.W.B Kibble, M.Krusius, Yu.G.Makhlin, B.Placais, G.E.Volovik and Wen Xu, “Vortex formation in neutron irradiated ^3He as an analogue of cosmological defect formation”, Nature **382**, 334 (1996).
- [55] Ü. Parts, J.M. Karimäki, J.H. Koivuniemi, M. Krusius, V.M.H. Ruutu, E.V. Thuneberg, and G.E. Volovik, “Phase diagram of vortices in superfluid $^3\text{He-A}$ ”, Phys. Rev. Lett. **75**, 3320 (1995).
- [56] G.E. Volovik, V.P. Mineev, “Current in superfluid Fermi liquids and the vortex core structure”, JETP **56**, 579 (1982)
- [57] G.E. Volovik, “Action for anomaly in fermi superfluids: quantized vortices and gap nodes”, JETP **77**, 435 (1993).
- [58] M.S. Turner, “Windows on the axion”, Phys. Rep. **197**, 67 (1990); J.E. Kim, “Cosmic Axion”, astro-ph/9802061.
- [59] S.L. Adler, “A strategy for a vanishing cosmological constant in the presence of scale invariance breaking”, Gen. Rel. Grav. **29** 1357 (1997).
- [60] A.A. Nersesyan, A.M. Tselik and F. Wenger, “Disorder effects in two-dimensional d -wave superconductors”, Phys. Rev. Lett., **72**, 2628 (1994).